

Demonstration of Real-Time Precision Optical Time Synchronization in a True Three-Node Architecture

Kyle W. Martin, Matthew S. Bigelow, *BlueHalo*

Nader Zaki, Benjamin K. Stuhl, Nolan Matthews, *Space Dynamics Laboratory*

John D. Elgin, Kimberly Frey, *Air Force Research Laboratory*

ABSTRACT

Multi-node optical clock networks will enable future studies of fundamental physics and enable applications in quantum and classical communications as well as navigation and geodesy. We implement the first ever multi-node optical clock network with real-time, relative synchronization over free-space communication channels and precision on the order of 10 fs, realized as a three-node system in a hub-and-spoke topology. In this paper we describe the system and its performance, including a new, independent, out-of-loop verification of two-way optical time synchronization.

I. INTRODUCTION

The most precise optical atomic clocks have now demonstrated frequency stability at levels that reach below 1×10^{-17} in only 1000 s (18; 5; 13; 7; 20; 23). Networks of these optical clocks could be utilized in studies of fundamental physics of relativity (8; 27), searches for ultralight (29) or topological dark matter (1; 10; 30; 14), gravitational wave detection (28; 16), and geodesy (19; 12). Furthermore, a system synchronized to this level has many applications, such as quantum networking (6), high rate data transfer over optical links (21), and global navigation satellite systems (24). However, to establish an optical clock network which achieves the fractional frequency stabilities individually realized by these clocks, there must exist a method of synchronization with performance even better than them. Additionally, high-performance synchronization systems have great value in distributing time from an ultra stable but bulky and power-hungry lattice or ion clock to a clock with lower size, weight, and power (SWaP) (2), to realize increased time and frequency stability in environments where low instability clocks could not otherwise operate.

There have been several demonstrations of time synchronization at the femtosecond level (i.e. time deviation (TDEV) in the single-digit femtosecond range from 1 s to 1 hour) over continuous links (25; 2; 11; 15; 3). Heretofore, these methods have only been demonstrated for a two-node point-to-point link, while many applications for an optical clock network require multiple nodes. Bodine *et al.* (4) made progress beyond a two-node, single-link system by constructing a mid-link relay and demonstrating that it did not degrade the overall performance. However, the relay was not itself synchronized or syntonized to the Primary node, and so did not actively participate in the timing network. Moreover, the two endpoints shared a common clock and so were only able to measure link noise rather than full synchronization. In what follows, we present results for the first demonstration of a true three-node, three-clock, free-space, real-time optical time synchronization network with femtosecond level performance.

II. NETWORK DESIGN

Our multi-node system, illustrated schematically in Fig. 1a, implements a hub-and-spoke topology where the central Primary node distributes time to two spatially-separated Secondary nodes; there is no optical time synchronization link between Secondary sites 1 and 2. In this experiment, all three nodes are located in the same laboratory, but each node is self-contained within a single electronics rack and each has an independent cavity-stabilized laser as shown in Fig. 1b. The experiment involved two independent free-space links set up on an optics table connected to each node by 10 m of fiber. The free-space path of the Primary to Secondary 1 node was approximately 11 m and Primary to Secondary 2 node was approximately 4 m. Additionally, direct comparison of the optical frequency combs at the Primary and Secondary nodes are performed in a 3 m out-of-loop verification fiber, depicted as the looped fiber between nodes in Fig. 1a.

We employ a similar two-way optical frequency comb-based time synchronization protocol to (25; 2; 11; 15; 3) using “linear optical sampling” or cross-correlation measurements from optical heterodyne beats between frequency comb pulses (9). Local comb A at the Primary site and remote combs Y and Z at the Secondary sites are each individually locked to a stable reference cavity laser such that the repetition rate of the combs are $f_{rep} \approx 200$ MHz. These three clock combs are the physical oscillators that are network-synchronized to the femtosecond level. Offset-repetition rate linear optical sampling requires an additional

frequency comb, referred to as the transfer comb, which is located at the Primary site and is locked with a slightly lower repetition rate $f_{rep} - \Delta f_{rep}$ where $\Delta f_{rep} \approx 2.08$ kHz. Comb pulses are exchanged between the transfer comb at the Primary site and the remote combs Y and Z at the Secondary sites over a free-space optical link and generate interferograms (IGMs) in the transceiver (Fig. 1c) at each node. IGMs are generated every $1/\Delta f_{rep} \approx 481$ μ s.

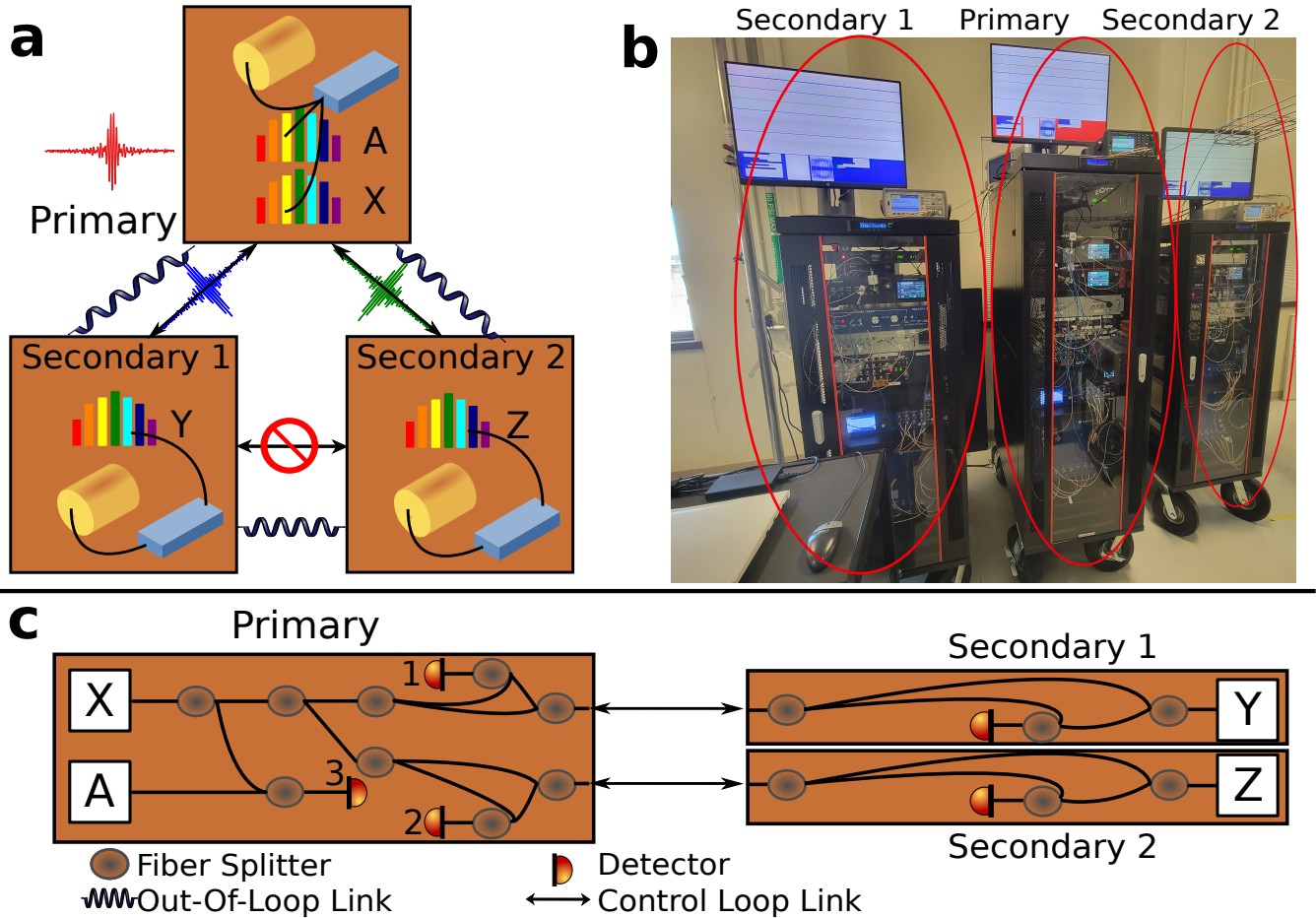


Figure 1: Optical frequency comb-based two-way time synchronization setup. **a** shows the free-space optical links. Light from the optical frequency combs at the Secondary nodes are optically mixed with the synchronization comb light producing interferograms (IGMs). The time of arrival of these IGMs is measured and the repetition rate of the optical frequency combs at each of the Secondary nodes is adjusted accordingly. These nodes are truly independent – note there is no direct free-space link, and thus no direct control, between the Secondary nodes. Also shown here is the out-of-loop measurement performed via a fiber link in which the optical frequency combs at both Secondary nodes are sent back to the Primary node and compared to comb A. Furthermore, combs Y and Z are compared at both nodes 1 and 2 in a separate verification measurement. **b** is a picture of our three-node time synchronization system. **c** shows a simplified diagram of the IGM generation.

Figure 1c shows a simplified optical setup of the two-way optical time synchronization experiment. At the Primary node light from the transfer comb X is split. One part is optically mixed with local comb A and detected on detector 3 generating the local/transfer IGM, while the remaining light from the transfer comb is then split again to be used separately for the two transceivers at the Primary site. In each transceiver, the transfer comb is split one last time reserving some of the light to be optically mixed with the received remote comb light, generating the remote/transfer IGM on detectors 1 and 2, while the majority of the light is sent over the free space optical links to each of the Secondary nodes. At each site the arrival time of the IGM is measured with respect to that site's local timebase, and the timestamps are then transmitted between sites over a free-space optical communications link co-propagating with the frequency comb pulses. The timestamps are mathematically combined to yield the time of flight between each site and the offset between each Secondary site's clock and the Primary site's clock. The Secondary site clock combs are adjusted through a real-time feedback controller to null the clock offsets by varying the lock offset frequency f_{opt} between the clock comb and the optical reference cavity.

Since the 200 MHz repetition rate of the frequency combs leads to a timing ambiguity modulo $1/f_{rep}$, we utilize a coarse timing link (11) for each Secondary node to overcome this 5 ns ambiguity. We send coarse timing information over the same free-space optical path that is used to transmit the frequency comb light; a waveguide electro-optic modulator is used to encode a pseudo random binary sequence on the phase of the continuous wave laser at 1531 nm. This optical communications link is also the channel used to exchange the timestamps of the linear optical sampling measurements (mentioned above) enabling closure of the time synchronization loop.

With any time synchronization experiment, it is important to characterize the performance using an out-of-loop verification technique. For two-node systems, a heterodyne method (11) has been employed to ascertain the level of synchronization between the Primary and Secondary node. While our implementation of a multi-node system also enables the same measurements for characterization, it also distinctively enables characterization of the performance of the two independent Secondary nodes which have no direct communication between them, as well as removes the concomitant dependency of the local clock from the characterization. In both the latter case and the standard two-node implementation, the two nodes being compared have their f_{ceo} 's offset by a fixed amount (1 MHz in our case). For perfect synchronization the beat note oscillates at a frequency given by this difference in f_{ceo} of the two frequency combs. Variations in the relative amplitude of the detected signal enable measurement and characterization of the level of precision of the time synchronization achieved in the system. We note that performing the verification measurements between the Primary node and both Secondary nodes, as well as between the two Secondary nodes, is analogous to three-corner-hat clock measurements in the sense that such a characterization of a three-node optical time synchronization experiment is more robust against unintended measurement bias.

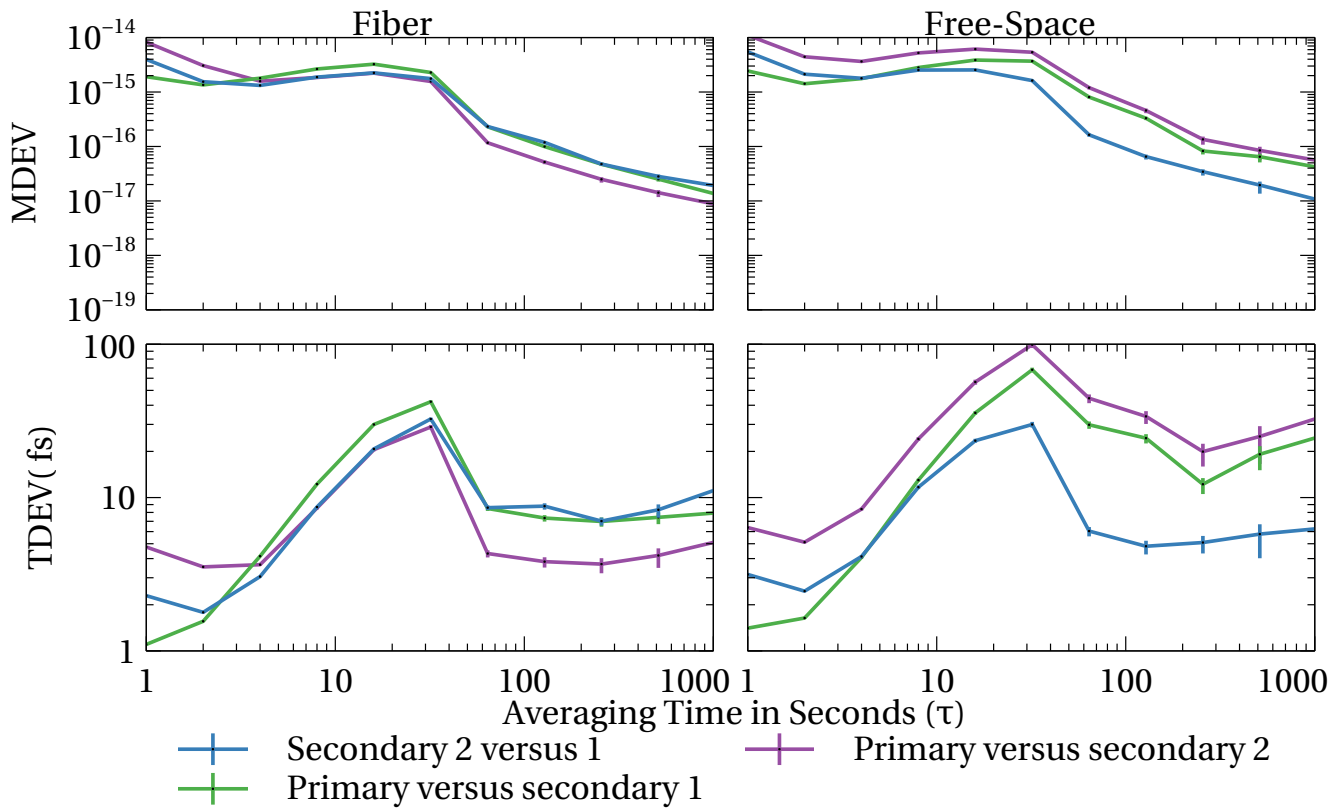


Figure 2: Shown above are the results from the three-node time synchronization experiment. We compare the Primary node to each Secondary node using the standard out-of-loop fiber link and observe the heterodyne of the frequency combs. We also observe the heterodyne between the two Secondary combs. Comb pulses were exchanged to synchronization time in both fiber and free-space. Both modified Allan deviation and time deviation measurements are shown for both fiber and free space links. The right two plots show the free-space experiments which were slightly noisier than the fiber experiments (shown on the left two plots). We also note that since the system is eventually designed to operate in three distinct locations, the out-of-loop verification fiber is much longer than normal and exposed to room temperature fluctuations resulting in excess noise on the verification data.

III. RESULTS

Utilizing the heterodyne out-of-loop verification technique described previously, we characterize the performance of the time synchronization protocol with modified Allan deviation (MDEV, $\text{mod } \sigma_y(\tau)$) and time deviation measurements (TDEV, $\sigma_x(\tau)$) over a few hours – first under direct fiber connections and then over short free-space links. The modified Allan deviation differs from the standard Allan deviation in that it numerically varies the measurement bandwidth depending on the averaging period τ . This variation of the binned time averaged phase measurements allows for the disambiguation of measurements with white phase noise and white frequency noise (17). After calculation of the modified Allan deviation the time deviation is simply given by $\sigma_x(\tau) = \frac{\tau}{\sqrt{3}} \text{mod } \sigma_y(\tau)$ (22).

Our results in Fig. 2 show TDEVs at 1 second at the femtosecond level for each of two independent links (Primary \leftrightarrow Secondary 1 and Primary \leftrightarrow Secondary 2), as well as similar precision for the out-of-loop comparison between the two Secondary nodes. Each data set (fiber link or free-space link) is collected under two separate initialization conditions. Data is first simultaneously collected between the clock combs at the Primary node and the two respective Secondary nodes; then the offset between the two Secondary node clock combs is re-adjusted to 1 MHz, and data is collected again but now between the two frequency combs at the Secondary sites.

We note that our out-of-loop measurements have excess noise relative to previously published two-node work. As reported in (26), the out-of-loop verification technique is susceptible to deviations in fiber path length (unlike the in-loop optical time synchronization protocol). In this experiment the nodes were tested in the same laboratory, but each node is fully self-contained and designed to be placed at a remote location relative to the others. This design results in the out-of-loop fiber being 3 m long which has added to the residual long-term measurement noise associated with temperature fluctuations over this link.

IV. DISCUSSION AND FUTURE WORK

We see opportunities to greatly increase the utility of this work. The hub-and-spoke topology used for this experiment keeps a centralized node that all other nodes are steered towards. A more robust topology would allow any individual node to become the Primary or Secondary node. Such a configuration would require an optical link between what are now the two Secondary nodes and the introduction of one additional frequency comb at each of these sites. In addition, optical switching will likely need to be implemented in order to determine which comb pulses are sent for the eventual heterodyne at each site. Further optimization and improvement on the quality and precision of time synchronization is also currently under investigation for the three-node system in the hub-and-spoke topology. Next steps also include increasing the length of the free-space optical links by moving the Secondary nodes away from the Primary while maintaining the out-of-loop verification, as well as performing measurements in non-laboratory environments.

ACKNOWLEDGEMENTS

Approved for public release; distribution is unlimited. Public Affairs release approval # AFRL-2023-5866.

REFERENCES

- [1] Arvanitaki, A., Huang, J. W., and Tilburg, K. V. (2015). Searching for dilaton dark matter with atomic clocks. *Phys. Rev. D*, 91:015015.
- [2] Bergeron, H., Sinclair, L., Swann, W., Nelson, C., Deschênes, J., Baumann, E., Giorgetta, F., Coddington, I., and NR, N. (2016). Tight real-time synchronization of a microwave clock to an optical clock across a turbulent air path. *Optica*, pages 441–447.
- [3] Bigelow, M. S., Guidice, R., Martin, K., Metcalf, A. J., and Lemke, N. (2019). Free-space optical time transfer between an atomic frequency standard and a simple optical clock. In *2019 Conference on Lasers and Electro-Optics (CLEO)*, pages 1–2.
- [4] Bodine, M. I., Ellis, J. L., Swann, W. C., Stevenson, S. A., Deschênes, J.-D., Hannah, E. D., Manurkar, P., Newbury, N. R., and Sinclair, L. C. (2020). Optical time-frequency transfer across a free-space, three-node network. *APL Photonics*, 5(7):076113.
- [5] Bothwell, T., Kedar, D., Oelker, E., Robinson, J. M., Bromley, S. L., Tew, W. L., Ye, J., and Kennedy, C. J. (2019). JILA sri optical lattice clock with uncertainty of 2.0×10^{-18} . *Metrologia*, 56(6):065004.
- [6] Burenkov, I. A., Semionov, A., Hala, Gerrits, T., Rahmouni, A., Anand, D., Li-Baboud, Y.-S., Slattery, O., Battou, A., and Polyakov, S. V. (2023). Synchronization and coexistence in quantum networks. *Opt. Express*, 31(7):11431–11446.
- [7] Campbell, S. L., Hutson, R. B., Marti, G. E., GOoban, A., Oppong, N. D., McNally, R. L., Sonderhouse, L., Robinson,

- J. M., Zhang, W., Bloom, B. J., , and Ye, J. (2017). A Fermi-degenerate three-dimensional optical lattice clock. *Science*, 358:90–94.
- [8] Chou, C. W., Hume, D. B., Rosenband, T., and Wineland, D. J. (2010). Optical clocks and relativity. *Science*, 329(5999):1630–1633.
- [9] Coddington, I., Swann, W. C., and Newbury, N. R. (2009). Coherent linear optical sampling at 15 bits of resolution. *Opt. Lett.*, 34(14):2153–2155.
- [10] Derevianko, A. and Pospelov, M. (2014). Hunting for topological dark matter with atomic clocks. *Nat. Phys.*, 10:933–936.
- [11] Deschênes, J.-D., Sinclair, L. C., Giorgetta, F. R., Swann, W. C., Baumann, E., Bergeron, H., Cermak, M., Coddington, I., and Newbury, N. R. (2016). Synchronization of distant optical clocks at the femtosecond level. *Phys. Rev. X*, 6:021016.
- [12] Grotti, J., Koller, S., Vogt, S., Häfner, S., Sterr, U., Lisdat, C., Denker, Heiner nad Voigt, C., Timmen, L., Rolland, A., Baynes, F. N., Margolis, H. S., Zampaolo, M., Thoumany, P., Pizzocaro, M., Rauf, B., Bregolin, F., Tampellini, A., Barbieri, P., Zucco, M., Costanzo, G. A., Clivati, C., Levi, F., and Calonico, D. (2018). Geodesy and metrology with a transportable optical clock. *Nature Physics*, 14:437–441.
- [13] Hinkley, N., Sherman, J. A., Phillips, N. B., Schioppo, M., Lemke, N. D., Beloy, K., Pizzacaro, M., Oates, C. W., and Ludlow, A. D. (2013). An atomic clock with 10^{-18} instability. *Science*, 341:1215–1218.
- [14] Kennedy, C. J., Oelker, E., Robinson, J. M., Bothwell, T., Kedar, D., Milner, W. R., Marti, G. E., Derevianko, A., and Ye, J. (2020). Precision metrology meets cosmology: Improved constraints on ultralight dark matter from atom-cavity frequency comparisons. *Phys. Rev. Lett.*, 125:201302.
- [15] Khader, I., Bergeron, H., Sinclair, L., Swann, W., Newbury, N., and Deschênes, J.-D. (2018). Time synchronization over a free-space optical communication channel. *Optica*.
- [16] Kolkowitz, S., Pikovski, I., Langellier, N., Lukin, M. D., Walsworth, R. L., and Ye, J. (2016). Gravitational wave detection with optical lattice atomic clocks. *Phys. Rev. D*, 94:124043.
- [17] Lesage, P. and Ayi, T. (1984). Characterization of frequency stability: Analysis of the modified allan variance and properties of its estimate. *IEEE Transactions on Instrumentation and Measurement*, 33(4):332–336.
- [18] Ludlow, A. D., Boyd, M. M., Ye, J., Peik, E., and Schmidt, P. O. (2015). Optical atomic clocks. *Rev. Mod. Phys.*, 87:637–701.
- [19] McGrew, W., Zhang, X., Fasano, R., Schäffer, S., Beloy, K., Nicolodi, D., Brown, R., Hinkley, N., Milani, G nad Schioppo, M., Yoon, T., and Ludlow, A. (2018). Atomic clock performance enabling geodesy below the centimetre level. *Nature*.
- [20] Oelker, E., Hutson, R. B., Kennedy, C. J., Sonderhouse, L., Bothwell, T., Goban, A., Kedar, D., Sanner, C., Robinson, J. M., Marti, G. E., Matei, D. G., Legero, T., Giunta, M., Holzwarth, R., Riehle, F., Sterr, U., and Ye, J. (2019). Demonstration of 4.8×10^{-17} stability at 1 s for two independent optical clocks. *Nature Photonics*, 13:714–719.
- [21] Okawachi, Y., Kim, B. Y., Lipson, M., and Gaeta, A. L. (2023). Chip-scale frequency combs for data communications in computing systems. *Optica*, 10(8):977–995.
- [22] Riley, W. and Howe, D. (2008). Handbook of frequency stability analysis.
- [23] Schioppo, M., Brown, R. C., McGrew, W. F., Hinkley, N., Fasano, R. J., Beloy, K., Yoon, T. H., Milani, G., Nicolodi, D., Sherman, J. A., Phillips, N. B., Oates, C. W., and Ludlow, A. D. (2017). Ultrastable optical clock with two cold-atom ensembles. *Nature Photonics*, pages 48–52.
- [24] Schuldt, T., Gohlke, M., Oswald, M., Wüst, J., Blomberg, T., Döringshoff, K., Bawamia, A., Wicht, A., Lezius, M., Voss, K., Krutzik, M., Herrmann, S., Kovalchuk, E., Peters, A., and Braxmaier, C. (2021). Optical clock technologies for global navigation satellite systems. *GPS Solutions*.
- [25] Sinclair, L. C., Bergeron, H., Swann, W. C., Khader, I., Cossel, K. C., Cermak, M., Newbury, N. R., and Deschênes, J.-D. (2019). Femtosecond optical two-way time-frequency transfer in the presence of motion. *Phys. Rev. A*, 99:023844.
- [26] Sinclair, L. C., Swann, W. C., Deschênes, J.-D., Bergeron, H., Giorgetta, F. R., Baumann, E., Cermak, M., Coddington, I., and Newbury, N. R. (2016). Optical system design for femtosecond-level synchronization of clocks. In *Slow Light, Fast Light, and Opto-Atomic Precision Metrology IX*, volume 9763, pages 11–26. SPIE.
- [27] Takamoto, M., Ushijima, I., Ohmae, N., Yahagi, T., Kokado, K., Shinkai, H., and Katori, H. (2020). Test of general relativity by a pair of transportable optical lattice clocks. *Nature Photonics*, 14:411–415.

- [28] Takano, T., Takamoto, M., Ushijima, I., Ohmae, N., Akatsuka, T., Yamaguchi, A., Kuroishi, Y., Munekane, H., Miyahara, B., and Katori, H. (2016). Geopotential measurements with synchronously linked optical lattice clocks. *Nature Photonics*, 10:662–666.
- [29] Tsai, Y.-D., Eby, J., and Safronova, M. S. (2023). Direct detection of ultralight dark matter bound to the sun with space quantum sensors. *Nature Astronomy*, 7(1):113–121.
- [30] Wcisło, P., Ablewski, P., Beloy, K., Bilicki, S., Bober, M., Brown, R., Fasano, R., Ciuryło, R., Hachisu, H., Ido, T., Lodewyck, J., Ludlow, A., McGrew, W., Morzyński, P., Nicolodi, D., Schioppo, M., Sekido, M., Targat, R. L., Wolf, P., Zhang, X., Zjawin, B., and Zawada, M. (2018). New bounds on dark matter coupling from a global network of optical atomic clocks. *Science Advances*, 4(12).